

# Ultra Fast Self-Compton Cooling

Kunihito Ioka

*Department of Earth and Space Science, Osaka University, Toyonaka 560-0043, Japan*

ioka@vega.ess.sci.osaka-u.ac.jp

## ABSTRACT

We investigate the synchrotron self-Compton process in a planar shell taking the shock structure into account. We find that the energy density of the seed photons could deviate from the one-zone estimate by order of unity depending on the shock velocity and the electron cooling time. We also find that as the electron cooling becomes faster, the seed photons are increased more, so that the inverse Compton cooling becomes more efficient. This “ultra” fast cooling may work in such as gamma-ray bursts, blazars and microquasars.

*Subject headings:* galaxies: jets — gamma rays: bursts — gamma rays: theory — radiation mechanisms: non-thermal — shock waves

## 1. INTRODUCTION

Relativistic shocks often arise in astrophysics when a faster flow hits upon a slower one such as in gamma-ray bursts (GRBs) (e.g., Piran 1999), blazars (e.g., Inoue & Takahara 1996; Kino, Takahara & Kusunose 2002; Rees 1978), microquasars (e.g., Mirabel & Rodríguez 1999; Levinson & Waxman 2001; Kaiser, Sunyaev & Spruit 2000) and so on. In the relativistic shocks, the kinetic energy of the flow turns into the internal one, and some fraction of the internal energy is distributed to electrons and magnetic fields. The electrons are accelerated in the shock front while the magnetic fields are amplified by the shock. Under these conditions, the accelerated electrons radiate nonthermal emission, such as synchrotron and inverse Compton (IC) emission. In this paper we will consider the synchrotron self-Compton (SSC) process, in which the seed photons for the IC emission are the synchrotron photons.

The intensity of the IC emission is proportional to the energy density of the seed photons (Rybicki & Lightman 1979). So far the energy density of the seed photons has been estimated from the one-zone argument (e.g., Inoue & Takahara 1996; Sari, Narayan & Piran 1996; Sari

& Esin 2001). In the one-zone model we assume that the seed photons are distributed uniformly over space. However the one-zone approximation is too crude at times. In fact the shock structure, such as the cooling layer (e.g., Granot, Piran & Sari 2000) or the magnetized layer (e.g., Rossi & Rees 2002), could bring new features. Also for the seed photons, the shock structure may be important since the uniformity is violated near the shock front. At least we should evaluate the validity of the one-zone approximation quantitatively taking the shock structure into account.

In this paper, we will investigate the effects of the shock structure on the energy density of the seed photons in the SSC process. Especially we will concentrate on the geometrical effects. We will find that for some parameters the energy density of the seed photons could deviate from the one-zone estimate by order of unity.

## 2. PLANAR MODEL

Let us consider the following simple model. Our model is not so sophisticated as the realistic ones. However simplicity should be helpful in elucidating the main features.

We consider an optically thin uniform shell with a thickness  $D$  and a shock propagating with a velocity  $c\beta = c(1 - \gamma^{-2})^{1/2}$  measured in the shocked fluid frame (see Fig. 1). Electrons are accelerated just behind the shock and the motion of the electrons is negligible in the shocked fluid frame, if the electron acceleration time is shorter than other timescales. To extract the geometrical effects, we assume that all particles and magnetic fields are isotropic in the shocked fluid frame. We consider only single scattering assuming that the higher order IC is suppressed by the Klein-Nishina effect.

Note that if the shock is strong and the shocked fluid is extremely hot, the shock velocity measured in the shocked fluid frame is given by  $\beta = [(\gamma_r - 1)/(\gamma_r + 1)]^{1/2}/3$  (Blandford & Mckee 1976), where  $\gamma_r \sim (\gamma_f/\gamma_s + \gamma_s/\gamma_f)/2$  is the relative Lorentz factor between the faster fluid with the Lorentz factor  $\gamma_f$  and the slower fluid with  $\gamma_s$ . When  $\gamma_f/\gamma_s \sim 2$  and  $\gamma_f/\gamma_s \gg 1$ ,  $\beta \sim 0.1$  and  $\beta = 1/3$ , respectively. Therefore we will consider the cases  $\beta = 0.1$  and  $\beta = 1/3$ .

The energy density of the seed photons at a point  $r = R$  is given by the integration of all synchrotron radiation from the accelerated electrons as

$$U_\gamma(t, r = R) = \frac{2\pi}{c} \int d\mu ds \frac{1}{4\pi} P\left(t - \frac{s}{c}, r\right), \quad (1)$$

where  $P(t, r)$  erg s<sup>-1</sup>cm<sup>-3</sup> is the synchrotron power at a time  $t$  and a position  $r$ ,  $\mu = \cos\theta$  and  $s > 0$  (see Fig. 1). Note that the retarded time  $t - s/c$  is used in equation (1). For

simplicity, we consider the monoenergetic injection of the electrons. Since we concentrate on the total energy density of the seed photons, we can regard these monoenergetic electrons as the electrons that contribute most of the radiation energy even for the power-law injection case. To extract the essence, we adopt the following simple form as the synchrotron power,

$$P(t, r) = A \left[ H \left( t - \frac{r}{c\beta} \right) - H \left( t - \frac{r}{c\beta} - \Delta t_{cool} \right) \right], \quad (2)$$

which means that electrons radiate with a constant power  $A \text{ erg s}^{-1} \text{ cm}^{-3}$  for a duration  $\Delta t_{cool}$  s since the shock has passed. This is sufficient for the following argument, since the synchrotron power is proportional to the square of the electron Lorentz factor (Rybicki & Lightman 1979) and hence the cooled electrons have a small contribution to the total energy density of the seed photons.

Equation (2) makes it possible to integrate equation (1) analytically. As shown in § A, during the electron emission,

$$0 < \tilde{t} \equiv t - \frac{R}{c\beta} < \Delta t_{cool}, \quad (3)$$

the energy density in equation (1) is given by

$$U_\gamma(t, R) = \frac{A}{2} \left[ \beta(\Delta t_{cool} - \tilde{t}) \ln \frac{(1 - \beta)(t - \Delta t_{cool})}{\beta(\Delta t_{cool} - \tilde{t})} + \frac{R}{c} \ln \frac{t}{t - \Delta t_{cool}} + \beta \tilde{t} \ln \frac{(1 + \beta)t}{\beta \tilde{t}} \right], \quad (4)$$

if

$$\tilde{t} > \Delta t_{cool} - \frac{(1 - \beta)R}{c\beta}, \quad (5)$$

and

$$\tilde{t} < \frac{(1 + \beta)(D - R)}{c\beta}, \quad (6)$$

are satisfied. If equations (3) and (6) are satisfied but equation (5) is not, we have

$$U_\gamma(t, R) = \frac{A}{2} \left[ \frac{R}{c} \ln \frac{ct}{R} + \beta \tilde{t} \ln \frac{(1 + \beta)t}{\beta \tilde{t}} \right]. \quad (7)$$

### 3. ENERGY DENSITY OF SEED PHOTONS

Let us consider the energy density of the seed photons when the shock is in the region  $0 < r < D$ . The shock crossing time is given by  $\Delta t_{dyn} = D/c\beta$ . We call the case  $f \equiv \Delta t_{dyn}/\Delta t_{cool} > 1$  fast cooling, and  $f < 1$  slow cooling.

First, let us consider the one-zone model. In fast cooling, electrons emit almost all energy before the shock crosses the shell, so that the energy density of the seed photons is given by

$$U_\gamma^{1zone} = \int_0^{\Delta t_{cool}} d\tilde{t} P(t, r) = A\Delta t_{cool}, \quad (8)$$

with equation (2). In slow cooling, electrons do not emit all the energy within  $\Delta t_{dyn}$ . The electrons radiate with a power  $A$  for a duration  $\Delta t_{dyn}$ , so that

$$U_\gamma^{1zone} = A\Delta t_{dyn} = \frac{AD}{c\beta}. \quad (9)$$

In the planar model, the energy density of the seed photons is given by equations (4) and (7). To compare the planar model with the one-zone model, we take the time and position average of the energy density,  $\langle U_\gamma(t, r) \rangle \equiv \int_0^D (dr/D) \int_0^{\Delta t} (d\tilde{t}/\Delta t) U_\gamma(t, r)$  where  $\Delta t \equiv \min[\Delta t_{cool}, (D - r)/c\beta]$ . In the fast cooling limit  $f \gg 1$ , we have

$$\langle U_\gamma(t, r) \rangle = \frac{\beta A \Delta t_{cool}}{2} \left[ \frac{1}{2} + \ln \frac{f}{\beta\gamma} \right]. \quad (10)$$

Note that the logarithmic term originates from the integral of  $\sim 1/\mu$ , i.e., the geometrical effect (see § A). In the slow cooling limit  $f \ll 1$ , we have

$$\langle U_\gamma(t, r) \rangle = \frac{AD}{24c} \left[ \pi^2 - 6 + 3 \ln \frac{1 + \beta}{\beta^3} \right]. \quad (11)$$

In Fig. 2 we show the ratio of the energy density of the seed photons to the one-zone estimate  $\langle U_\gamma(t, r) \rangle / U_\gamma^{1zone}$  for  $\beta = 1/3$  and  $\beta = 0.1$ . The analytical approximations in equations (10) and (11) are also shown by dashed lines. We see that the analytical approximations are quite good.

From Fig. 2, we can find the following features. First, for some parameters, e.g.,  $\beta = 0.1$  and  $f \lesssim 1$ , the energy density of the seed photons deviates from the one-zone estimate by order of unity. Second, the dependence of the energy density on the shock velocity  $c\beta$  differs between in the planar model and the one-zone model. Finally, in fast cooling the energy density of the seed photons increases as the ratio  $f$  increases, because of the logarithmic term in equation (10). This is an interesting new feature due to the geometrical effect. Increasing the seed photons enhances the IC emission and hence the IC cooling. Therefore this mechanism may be termed “ultra” fast cooling. The difference between  $f = 1$  and  $f \sim 10^6$  is about order of unity when  $A\Delta t_{cool} = \text{const}$ . Surprisingly the energy density of the seed photons can be larger than that of the electrons which supply the seed photons.

To make the physical situation clear, the region from which photons come is shade in Fig. 3. Here we assume that equations (3), (5) and (6) are satisfied. This causal region is bounded by four constraints as in Fig. 4 (see § A), (a)  $s = R/\mu$ , (b)  $s = -(D - R)/\mu$ , (c)  $s = (c\beta t - R)/(\beta - \mu)$  and (d)  $s = [c\beta(t - \Delta t_{cool}) - R]/(\beta - \mu)$ . The boundary (c) represents the hyperboloid of two sheets,

$$\frac{x^2 + y^2}{\gamma^2 c^2 \beta^2 \tilde{t}^2} - \frac{(r - R - \gamma^2 c \beta \tilde{t})^2}{\gamma^4 c^2 \beta^4 \tilde{t}^2} = -1, \quad (12)$$

where  $x^2 + y^2 = s^2(1 - \mu^2)$ . The boundary (d) is also described by equation (12) with  $\tilde{t}$  replaced by  $\tilde{t} - \Delta t_{cool}$ . From equation (12) we can see that the photons approximately come from the direction  $\sim \tan \theta = \beta^{-1}\gamma^{-1}$ . This is physically reasonable since the cooling layer for fast cooling is very close to the shock front and the shock front has the same velocity towards the  $r$ -axis as the photons traveling in the direction of  $\tan \theta = \beta^{-1}\gamma^{-1}$ . In a sense, photons are accumulated around the shock front as the shock sweeps. The approximation of the planar shell is valid when the size of the shell is larger than  $\sim \beta^{-1}\gamma^{-1}D$ .

#### 4. APPLICATIONS

(I) In the internal shocks of the GRBs (e.g., Piran 1999; Sari, Narayan & Piran 1996), the cooling time of electrons is about  $\Delta t_{cool} \sim 6\pi\gamma_e m_e c^2 / \sigma_T c \gamma_e^2 B^2 \sim 10^{-6} \gamma_{e,3}^{-1} B_6^2$  s, where  $\gamma_e = 10^3 \gamma_{e,3} \sim m_p/m_e$  is the Lorentz factor of the electrons which contribute most of the radiation energy, and  $B = 10^6 B_6$  G is the magnetic field. The shock crossing time is about  $\Delta t_{dyn} \sim \Gamma d/c \sim 1\Gamma_2 d_8$  s, where  $\Gamma = 10^2 \Gamma_2$  is the Lorentz factor of the shell and  $d = 10^8 d_8$  cm is the shell thickness in the lab frame. A large dispersion of the Lorentz factors may be needed for the efficient internal shock (Beloborodov 2000; Kobayashi & Sari 2001). Thus  $\beta \sim 1/3$  and  $f = \Delta t_{dyn}/\Delta t_{cool} \sim 10^6$ . From Fig. 2, the energy density of the seed photons is larger than the one-zone estimate by a factor of  $\sim 3$ .

(II) The late afterglows of the GRBs are likely in the slow cooling regime (Sari & Esin 2001). Most of the radiation energy is emitted by electrons with  $f = 1$ . For the forward shock the shock velocity is  $\beta \sim 1/3$ , while for the reverse shock the shock velocity has various values depending on the parameters (Sari & Piran 1995). From Fig. 2, the one-zone estimate may overestimate the energy density of the seed photons by order of unity for  $\beta = 0.1$ .

(III) In the TeV blazars, most of the radiation is emitted by electrons with the maximum Lorentz factor  $\gamma_{max} \sim 10^5$  if the power law index of the electron distribution is  $s < 2$  (see Kino, Takahara & Kusunose 2002). Since electrons with the break Lorentz factor  $\gamma_{br} \sim 10^3$  corresponds to the electrons with  $f = 1$  and the cooling time is proportional to the inverse

of the electron Lorentz factor, the electrons with  $\gamma_{max}$  have  $f \sim 10^2$ . If we take the Klein-Nishina effect into account, photons emitted by the electrons with  $\gamma_{max}$  cannot be seed photons for the electrons with  $\gamma_{max}$ . In this case  $f$  is reduced to  $f \sim 10$  or so. If the emission arises from the internal shock with the relative Lorentz factor  $\gamma_r \sim 2$  (Rees 1978),  $\beta \sim 0.1$ . From Fig. 2, the one-zone estimate may overestimate the energy density of the seed photons by a factor of  $\sim 4$ .

(IV) In the microquasars, according to Levinson & Waxman (2001), the ratio of the shock crossing time to the cooling time is about  $f \sim 10^5 l_8^{-1}$  where  $l$  is the collision radius of the internal shock. If we take the Klein-Nishina effect into account in the case  $l_8 = 1$ ,  $f$  is reduced to  $f \sim 10^4$  or so. If the relative Lorentz factor between shells is  $\gamma_r \sim 2$ ,  $\beta \sim 0.1$ . From Fig. 2, if  $l = 10^8$  cm, the one-zone estimate is correct within a factor of 2, while if  $l = 10^{13}$  cm, the one-zone estimate may overestimate the energy density of the seed photons by order of unity.

## 5. DISCUSSIONS

We have not dealt with the emission spectrum since we concern the total energy density in this paper. If we consider the energy distribution of electrons, the ultra fast cooling may modify the emission spectrum conventionally used in the one-zone model. This is because the cooling time depends on the electron energy, i.e., less energetic electrons cool slower. As expected from our analyses, the seed photon field that electrons feel will depend on the cooling time of the electrons. Therefore the spectrum of the IC emission should be modified, since the seed photon density is independent of the electron cooling time in the one-zone model. Furthermore if the IC cooling dominates the synchrotron one, the well known fact that the energy distribution of the cooled electrons breaks by one power in the index (e.g., Heavens & Meisenheimer 1987) should be modified because of the same reason. Detail studies will be presented in the future paper.

To be precise, when the IC cooling dominates, we have to solve the electron cooling together with equation (1). This problem is the one-dimensional radiative transfer with the electron cooling. We may be able to solve this problem numerically, although a large memory will be necessary for resolving the cooling layer in fast cooling.

We may have to consider other effects. For example, the approximation of the uniform shell may not be good. The reverse shock emission and the deceleration of the shock may be important. If the synchrotron power is not constant but a function of the distance from the center, the logarithmic correction may become a power law one. These are interesting

future problems.

I am grateful F. Takahara and M. Kino for useful comments. This work was supported in part by Grant-in-Aid for Scientific Research of the Japanese Ministry of Education, Culture, Sports, Science and Technology, No.00660.

### A. INTEGRATION IN EQUATION (1)

In Fig. 4, the region to be integrated in equation (1) is shaded. There are four constraints on the integral in equation (1), which are shown by solid lines in Fig. 4. (a)  $s < R/\mu$  since the shell has an end  $r = R - s\mu > 0$  and we consider  $R > 0$ . (b)  $s < -(D - R)/\mu$  since the shell has an end  $r = R - s\mu < D$  and we consider  $R < D$ . (c)  $s < (c\beta t - R)/(\beta - \mu)$  since the first Heaviside step function in equation (2) has to be unity at the retarded time  $t - s/c$ , i.e.,  $t - s/c - (R - s\mu)/c\beta > 0$ . (d)  $s < [c\beta(t - \Delta t_{cool}) - R]/(\beta - \mu)$  since the second step function in equation (2) has to be zero at the retarded time  $t - s/c$ , i.e.,  $t - \Delta t_{cool} - s/c - (R - s\mu)/c\beta < 0$ . Here we consider the interval during which electrons are emitting in equation (3), so that the line (c) is in the region  $\mu < \beta$  and the line (d) is in  $\mu > \beta$  as in Fig. 4. The lines (a) and (d) cross in the region  $\beta < \mu < 1$  as in Fig. 4 if equation (5) is satisfied, and vice versa. The lines (b) and (c) do not cross in the region  $-1 < \mu < 0$  as in Fig. 4 if equation (6) is satisfied, and vice versa. If equations (3), (5) and (6) are satisfied, equation (1) can be integrated as

$$U_\gamma(t, R) = \frac{A}{2c} \left[ \int_{R/c(t-\Delta t_{cool})}^1 d\mu \frac{c\beta(t - \Delta t_{cool}) - R}{\beta - \mu} + \int_{R/ct}^{R/c(t-\Delta t_{cool})} d\mu \frac{R}{\mu} + \int_{-1}^{R/ct} d\mu \frac{c\beta t - R}{\beta - \mu} \right], \quad (\text{A1})$$

which gives equation (4). If equations (3) and (6) are satisfied but equation (5) is not, we have

$$U_\gamma(t, R) = \frac{A}{2c} \left[ \int_{R/ct}^1 d\mu \frac{R}{\mu} + \int_{-1}^{R/ct} d\mu \frac{c\beta t - R}{\beta - \mu} \right], \quad (\text{A2})$$

which gives equation (7).

### REFERENCES

Beloborodov, A. M. 2000, ApJ, 539, L25

- Blandford, R. D., & Mckee, C. F. 1976, *Phys. Fluids*, 19, 1130
- Granot, J., Piran, T., & Sari, R. 2000, *ApJ*, 534, L163
- Heavens, A. F., & Meisenheimer, K. 1987, *MNRAS*, 225, 335
- Inoue, S., & Takahara, F. 1996, *ApJ*, 463, 555
- Kaiser, C. R., Sunyaev, R., & Spruit, H., C. 2000, *A&A*, 356, 975
- Kino, M., Takahara, F., & Kusunose, M. 2002, *ApJ*, 564, 97
- Kobayashi, S., & Sari, R. 2001, *ApJ*, 551, 934
- Levinson, A., & Waxman, E. 2001, *Phys. Rev. Lett.*, 87, 171101
- Mirabel, I. F., & Rodríguez, L. F. 1999, *ARA&A*, 37, 409
- Piran, T. 1999, *Phys. Rep.*, 314, 575
- Rees, M. 1978, *MNRAS*, 184, 61P
- Rossi, E., & Rees, M. J. 2002, *astro-ph/0204406*
- Rybicki, G. B., & Lightman, A., P. 1979, *Radiative Processes in Astrophysics* (New York: Wiley Interscience)
- Sari, R., & Esin, A. A. 2001, *ApJ*, 548, 787
- Sari, R., & Piran, T. 1995, *ApJ*, 455, L143
- Sari, R., Narayan, R., & Piran, T. 1996, *ApJ*, 473, 204



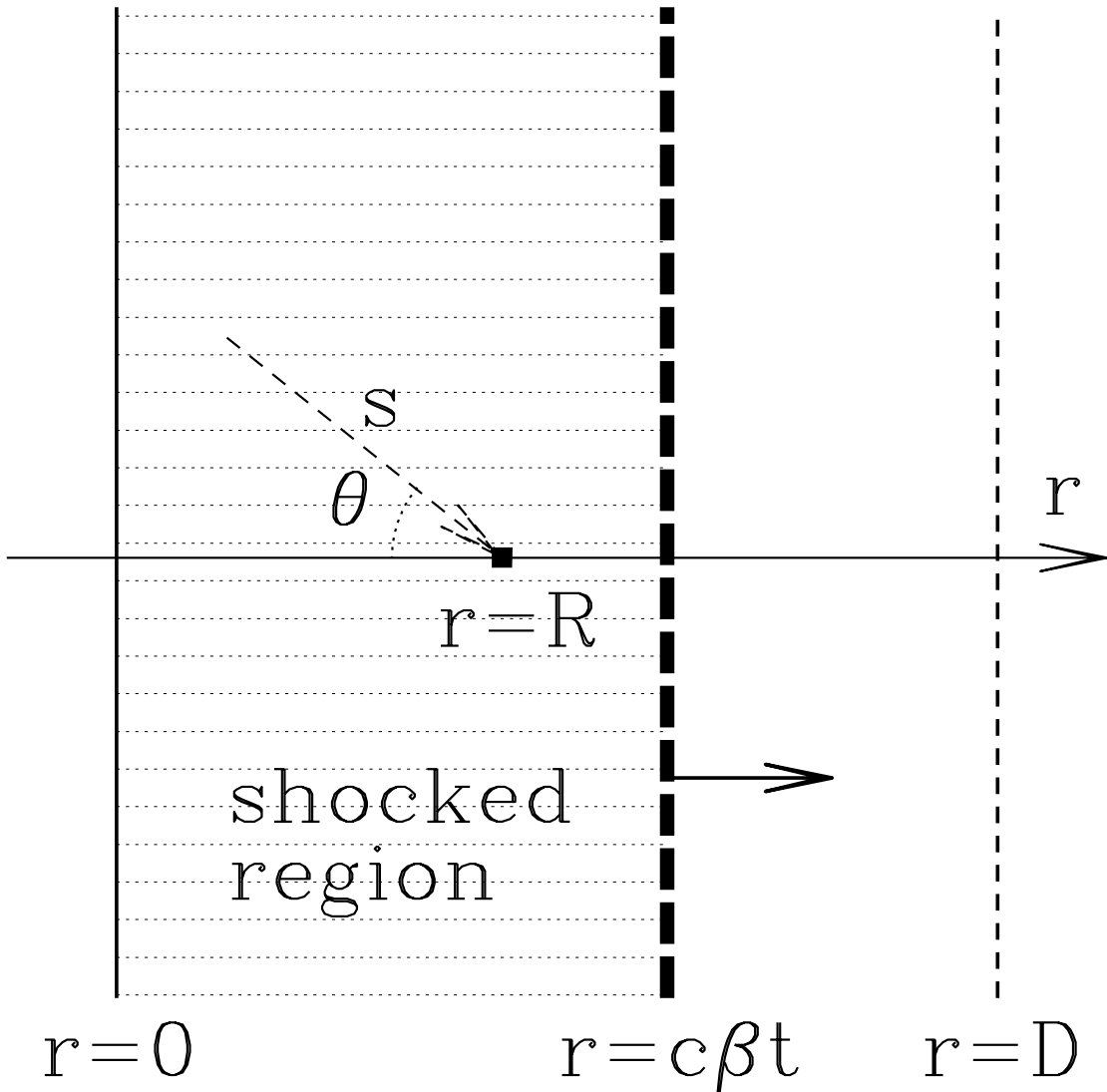


Fig. 1.— Our simple model is shown. We consider an optically thin uniform shell with a thickness  $D$  and a shock propagating with a velocity  $c\beta = c(1 - \gamma^{-2})^{1/2}$  measured in the shocked fluid frame. Electrons are accelerated just behind the shock, and then they cool radiating synchrotron and Compton emission. The motion of the electrons is neglected in the shocked fluid frame.

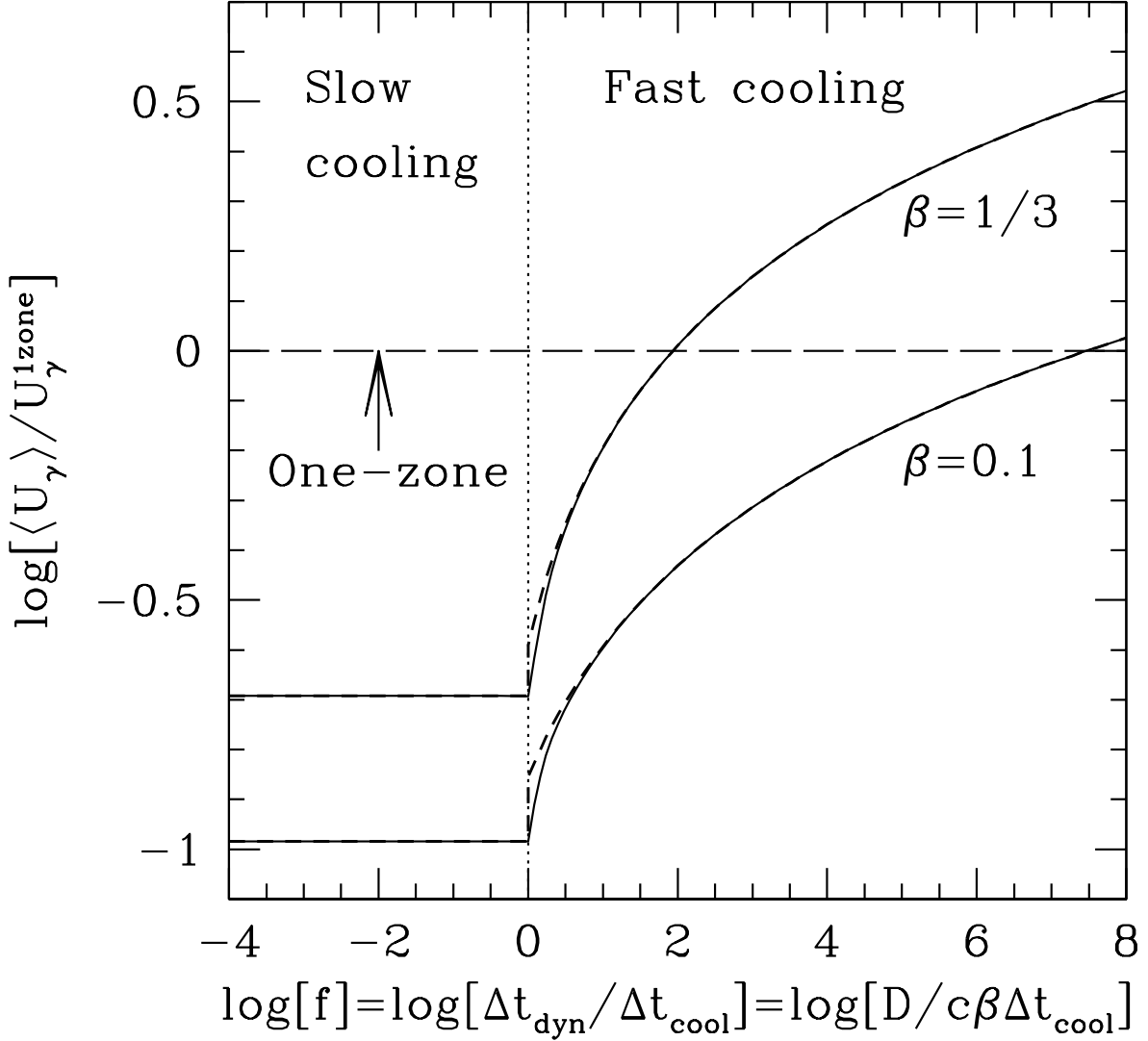


Fig. 2.— The energy density of the seed photons divided by the one-zone estimate  $\langle U_\gamma \rangle / U_\gamma^{1zone}$  as a function of the ratio of the shell crossing time to the electron cooling time  $f = \Delta t_{dyn} / \Delta t_{cool} = D / c\beta\Delta t_{cool}$  is shown for the shock velocities  $\beta = 1/3$  and  $\beta = 0.1$  with solid lines. The analytical approximations in equations (10) and (11) are also shown by dashed lines. We call  $f > 1$  fast cooling and  $f < 1$  slow cooling.

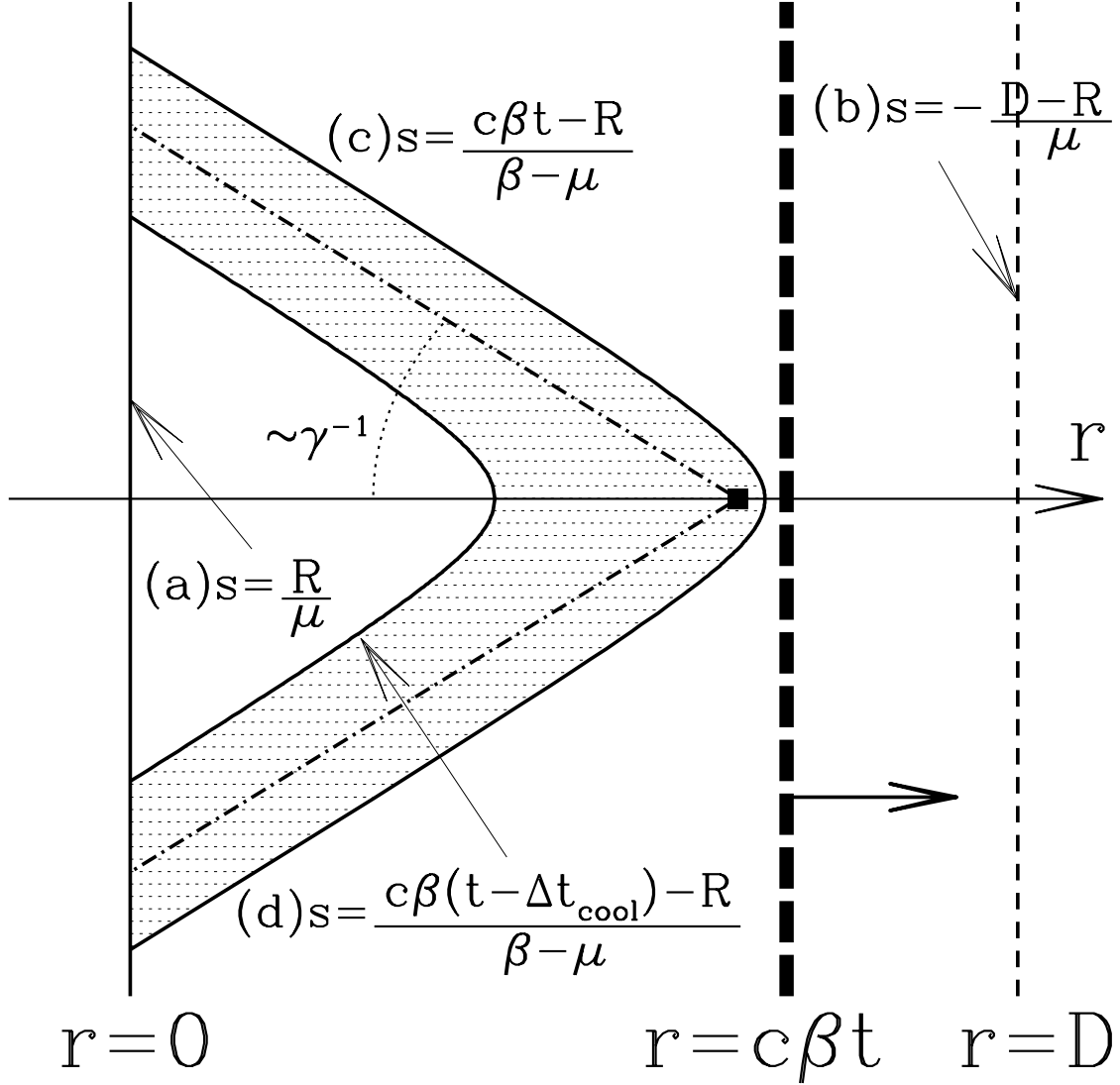


Fig. 3.— The region from which photons come to the square point is shaded (see also Fig. 1), where we assume that equations (3), (5) and (6) are satisfied. This causal region is bounded by four constraints as in Fig. 4, (a)  $s = R/\mu$ , (b)  $s = -(D - R)/\mu$ , (c)  $s = (c\beta t - R)/(\beta - \mu)$ , and (d)  $s = [c\beta(t - \Delta t_{cool}) - R]/(\beta - \mu)$ . The boundaries (c) and (d) are the hyperboloid of two sheets. The boundary (b) is not relevant to this figure. Approximately, photons come from the direction  $\tan \theta = \beta^{-1}\gamma^{-1}$ , which is shown by the dot-dashed lines.

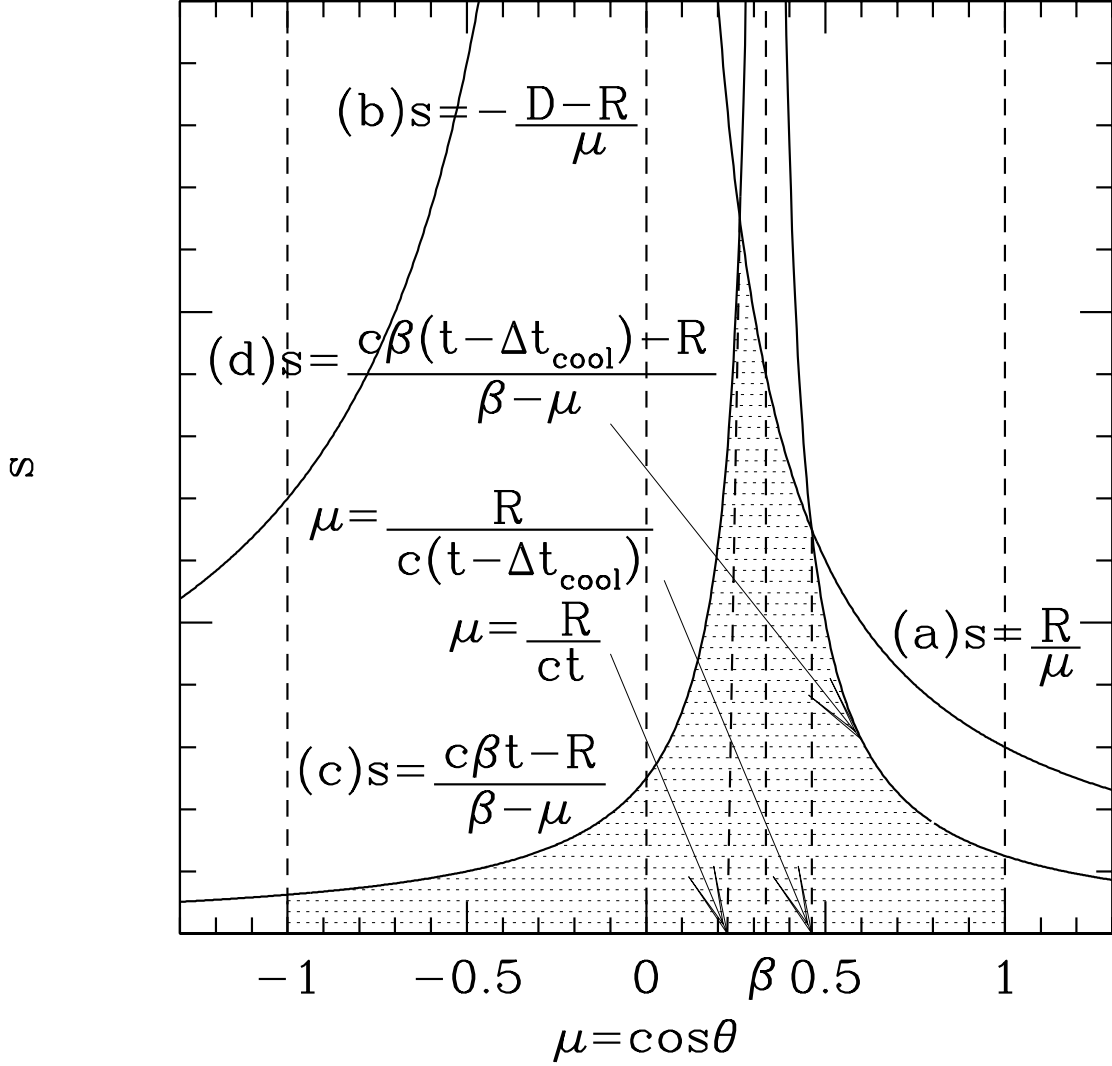


Fig. 4.— The region to be integrated in equation (1) is shaded in the  $(\mu, s)$  plane. Here we assume that equations (3), (5) and (6) are satisfied. Four constraints on the integral are shown by solid lines, (a)  $s = R/\mu$ , (b)  $s = -(D - R)/\mu$ , (c)  $s = (c\beta t - R)/(\beta - \mu)$  and (d)  $s = [c\beta(t - \Delta t_{cool}) - R]/(\beta - \mu)$ . The lines (a) and (c) cross at  $\mu = R/ct$ , and the lines (a) and (d) cross at  $\mu = R/c(t - \Delta t_{cool})$ .